UNCLASSIFIED MASTER COPY - FOR REPRODUCTION PURPOSES (2)

AD-A204 442

REPORT DOCUMENTATION PAGE

DTIC FILE COPY

Unclassified	1b. RESTRICTIVE MARKINGS
2a. SECURITY CLASSIFICATION AUTHORITY	3. DISTRIBUTION / AVAILABILITY OF REPORT
2b. DECLASSIFICATION / DOWNGRADING SCHEDULE	Approved for public release; distribution unlimited.
4. PERFORMING ORGANIZATION REPORT NUMBER(S)	5. MONITORING ORGANIZATION REPORT NUMBER(S)
	ARO 24076.6-EG
6a. NAME OF PERFORMING ORGANIZATION: University of Michigan	6b. OFFICE SYMBOL (If applicable)
7a. NAME OF MONITORING ORGANIZATION: U. S. Army Research Office	
6c. ADDRESS (City, State, and ZIP Code): University of Michigan, Ann Arbor, MI 48104	7b. ADDRESS (City, State, and ZIP Code): P. O. Box 12211, Research Triangle Park, NC 27709-2211
8a. NAME OF FUNDING / SPONSORING ORGANIZATION: U. S. Army Research Office	8b. OFFICE SYMBOL (If applicable)
9. PROCUREMENT INSTRUMENT IDENTIFICATION NUMBER: DAAL03-86-K-0154	
8c. ADDRESS (City, State, and ZIP Code): P. O. Box 12211, Research Triangle Park, NC 27709-2211	10. SOURCE OF FUNDING NUMBERS

PROGRAM ELEMENT NO.	PROJECT NO.	TASK NO.	WORK UNIT ACCESSION NO.

11. TITLE (Include Security Classification)

Separated-Flow Considerations for Pressure-Atomized Combusting Monopropellant Sprays

12. PERSONAL AUTHOR(S)

Gerard M. Faeth

13a. TYPE OF REPORT	13b. TIME COVERED FROM _____ TO _____	14. DATE OF REPORT (Year, Month, Day)	15. PAGE COUNT
Reprint			

16. SUPPLEMENTARY NOTATION

The view, opinions and/or findings contained in this report are those of the author(s) and should not be construed as an official Department of the Army position, policy, or decision, unless so designated by other documentation.

17. COSATI CODES			18. SUBJECT TERMS (Continue on reverse if necessary and identify by block number)
FIELD	GROUP	SUB-GROUP	

19. ABSTRACT (Continue on reverse if necessary and identify by block number)

Abstract on Reprint

DTIC ELECTE FEB 16 1988 S D Ca H

20. DISTRIBUTION / AVAILABILITY OF ABSTRACT ☐ UNCLASSIFIED/UNLIMITED ☐ SAME AS RPT. ☐ OTIC USERS	21. ABSTRACT SECURITY CLASSIFICATION: Unclassified
22a. NAME OF RESPONSIBLE INDIVIDUAL	22b TELEPHONE (Include Area Code) / 22c. OFFICE SYMBOL

DD FORM 1473, 84 MAR 83 APR edition may be used until exhausted. All other editions are obsolete.

SECURITY CLASSIFICATION OF THIS PAGE

UNCLASSIFIED

AIAA '89

AIAA 89-0049
Separated Flow Considerations for Pressure Atomized Combusting Monopropellant Sprays

T. Lee, L. Tseng and G. Faeth, Univ. of Michigan, Ann Arbor, MI

27th Aerospace Sciences Meeting
January 9–12, 1989/Reno, Nevada

SEPARATED-FLOW CONSIDERATIONS FOR PRESSURE-ATOMIZED COMBUSTING MONOPROPELLANT SPRAYS

AIAA-89-0049

T.-W. Lee,* L.-K. Tseng,* and G.M. Faeth†
The University of Michigan, Ann Arbor, Michigan

Abstract

The drop and spray combustion properties of the HAN-based monopropellant LGP 1845 were studied. Drop burning rates were measured with drops supported in a combustion gas environment at pressures of 0.2-7.0 MPa. Some internal gasification of drops -- causing swelling, partial bursting, and microexplosions -- was observed throughout this region but these disturbances decreased with increasing pressure. Effective drop burning rates (including effects of both surface gasification and bursting) were relatively constant, ca. 10 mm/s, and were consistent with earlier strand burning rate measurements of gelled propellant. Pressure-atomized combusting sprays were studied in combustion gas environments at pressures of 3-9 MPa. The liquid-containing region was significantly larger than earlier measurements of Birk and Reeves, as well as predictions based on the locally-homogeneous-flow approximation of multiphase flow theory. In conjunction with drop trajectory calculations, based on present measurements of drop burning rates, these findings suggest significant effects of separated flow in combusting HAN-based monopropellant sprays.

Nomenclature

C_D	= drop drag coefficient
d	= injector diameter
d_p	= drop diameter
k	= turbulence kinetic energy
K_p	= drop burning rate
L	= length of injector passage
Oh	= Ohnesorge number
p	= pressure
r	= radial distance
r_p	= drop radius
Re	= Reynolds number
t	= time
u	= streamwise velocity
We	= Weber number
x	= streamwise distance
α_f	= liquid volume fraction
ε	= rate of dissipation of turbulence kinetic energy
μ	= viscosity
ρ	= density
σ	= surface tension

Subscripts

c	= centerline value
f	= liquid-phase property
g	= gas-phase property
p	= drop property
o	= injector exit condition
∞	= ambient condition

Superscripts

$(\bar{\cdot})$	= time-averaged property
$(\tilde{\cdot})$	= Favre-averaged property

Introduction

Combusting monopropellant sprays have applications to regenerative liquid-propellant guns, throttable thrustors, and underwater propulsion systems. The objective of the present study was to experimentally investigate aspects of monopropellant spray combustion, seeking to extend earlier theoretical results obtained in this laboratory.[1-3] Two spray processes were considered, as follows: (1) the combustion properties of individual drops supported in combustion gas environments at pressures of 0.2-7.0 MPa; and (2) the structure of pressure-atomized combusting sprays in combustion gas environments at pressures of 3-9 MPa. The new measurements were used to assess the importance of separated-flow phenomena within pressure-atomized combusting monopropellant sprays, i.e., effects of finite relative velocities and transport rates between the phases. Similar to our earlier work,[1-3] the investigation was limited to a hydroxyl-ammonium nitrate (HAN)-based monopropellant (LGP 1845) which is of interest for several high-pressure monopropellant combustion systems.

Individual drop burning rates are needed for fundamental consideration of the properties of combusting monopropellant sprays. Earlier studies relevant to drop burning rates of HAN-based monopropellants have included measurements of strand burning rates[4-6] and the burning rates of individual drops in heated environments.[7-11] McBratney[4,5] measured strand burning rates of HAN-based monopropellants at pressures of 7-100 MPa. The propellant liquid was gelled with 2 weight percent Kelzan in order to stabilize turbulent-like disturbances of the liquid surface that are normally encountered during strand combustion tests at high pressures. The strand burning rates of gelled LGP 1845 were high (ca. 20 mm/s) and the pressure dependence was relatively weak (ca. $p^{0.1}$). A frothy region was observed at low pressures, where the thermal disturbance of the combustion wave extends an appreciable distance into the unburned propellant, suggesting significant reaction in the condensed phase for these conditions. While these results are valuable, however, the use of a gelling agent raises questions concerning its influence on the process. Vosen[6] measured strand burning rates of two ungelled HAN-based monopropellants, LGP 1846 and a 9.1 molar solution of HAN and water, at pressures of 7-30 MPa. The burning rates of both propellants were very high, 100-250 mm/s, and liquid surfaces were clearly disturbed, indicative of turbulent-like instability of burning liquid strands normally seen at high pressures; therefore, these results are difficult to interpret to find the fundamental combustion properties of the propellants.

Zhu and Law[7] studied the drop combustion properties of LGP 1845 and other HAN-based propellants, in combustion gases at 1170 K and 1 atm. The drops were observed to heat up with no radius change at first, then gasify from the surface for a time (with surface regression rates of ca. 0.2 mm/s), and finally burst when the drop diameter had decreased by roughly 15 percent. Beyer[8,9] and Beyer and Teague[10] studied the combustion of LGP 1846 drops supported in nitrogen at temperatures of 570-920 K and pressures of 0.1-8.2 MPa. These observations yielded results similar to Zhu and Law:[7] after a heat-up time and a period of relatively slow surface gasification (0.2 mm/s at 730 K and 1 MPa) the drops often burst -- particularly the larger drops. Both sets of drop experiments suggest that bulk liquid reaction and microexplosions may be important for combustion of HAN-based monopropellants but drop environment tempera-

* Graduate Assistant, Aerospace Engineering
† Professor, Aerospace Engineering, Fellow, AIAA

tures were low in comparison to the adiabatic combustion temperature of the monopropellant, (ca. 2150 K); therefore, the drops may not have ignited in a manner representative of spray combustion.

Earlier theoretical work in this laboratory addressed liquid surface and spray properties of combusting HAN-based monopropellants.[1-3] Analysis of liquid surface properties,[1,2] indicated relatively high liquid surface temperatures (in the range 800 - 1050 K for pressures greater than 10 MPa) and unusually high pressures for the liquid surface to reach its thermodynamic critical point (250 MPa with an estimated uncertainty of 50 percent). The high surface temperatures of the liquid surface provides greater potential for significant effects of chemical reaction in the bulk liquid than most monopropellants, helping to explain observations of microexplosions reported in Refs. 7-10. Furthermore, the high critical combustion pressure suggests that spray combustion of HAN-based monopropellants involves subcritical combustion with a drop-containing combusting spray for most applications.

The earlier analysis of combusting HAN-based monopropellant sprays,[1,3] was based on the locally-homogeneous-flow (LHF) approximation of multiphase flow theory, i.e., the assumption that velocity differences between the phases are negligible at each point in the flow;[11-13] and the thin laminar flamelet approximation of turbulent premixed flame theory, proposed by Bray.[14,15] Turbulent mixing was estimated using a Favre-averaged k-ε turbulence model, with empirical constants established from measurements in noncombusting variable-density round jets,[16,17] however, the constants used are very similar to early proposals based on constant-density turbulent flows.[18] The performance of the analysis was evaluated using the measurements of Birk and Reeves[19] for pressure atomized combusting LGP 1846 sprays at pressures of 6-8 MPa. There was encouraging agreement between predictions and measurements, however, predictions were very sensitive to the degree of flow development at the injector exit which was not known very well; therefore, this assessment was not definitive. Later measurements of noncombusting pressure-atomized sprays by Ruff et al.[13] established the strong sensitivity of spray properties to the degree of flow development at the jet exit and observed reasonably good performance of LHF analysis in the dense-spray region (liquid volume fractions greater than 0.2) near the injector exit for atomization breakup. However, these measurements also disclosed significant deficiencies of LHF analysis for other breakup regimes and in the dilute portion of the spray -- the last being in general agreement with other recent evaluations of the LHF approach for dilute sprays.[11,12]

The present investigation sought to extend past work concerning both drop and spray combustion of HAN-based monopropellants. Drop combustion was observed using an approach similar to Beyer[10] for pressures of 0.2-7 MPa, however, the drop environment more closely matched the gas temperature of a combusting monopropellant spray. Measurements of spray properties were undertaken seeking to confirm the measurements of Birk and Reeves,[19] while considering a broader range of experimental conditions at pressures of 3-9 MPa. The new spray measurements, in conjunction with both LHF analysis and drop trajectory calculations based on the present drop burning rate measurements, were used to assess the importance of separated-flow phenomena for these flows.

Drop Combustion

Experimental Methods

Apparatus. Figure 1 is a sketch of the drop combustion test apparatus. The supported-drop technique was used with the drops exposed to gases in the post-flame region of a premixed burner which was operated within a pressure vessel. The pressure vessel had an inside diameter and length of 130 and 430 mm and was fitted with two 25 mm diameter quartz windows so that the drops could be observed.

The premixed burner had a diameter of 10 mm with a stainless steel screen (0.17 mm diameter wires, 2000 wires/m, square pattern) to help stabilize the flame. The gas flow rates of the premixed burner were metered and controlled with critical flow orifices and pressure regulators. Burner operating times were short, just sufficient to stabilize the premixed flame and complete the drop combustion test. Burner gas flows were initiated and terminated with solenoid valves while the burner was ignited with an exploding wire. The pressure rise of the chamber (measured with a pressure transducer) was small in the period when the burner was operating, ca. 5 percent; therefore, the chamber pressure was set by backfilling it with air. The properties of the post-flame region of the premixed burner roughly approximated the temperatures of adiabatic combustion of the monopropellant, but contained significantly lower concentrations of water vapor, see Table 1 for the combustion product properties of LGP 1845 and the burner gases (denoted burner 1 and 2).

The drop support assembly is illustrated in Fig. 2. The drops were mounted on quartz fibers, 50-150 μm in diameter, with the bottom end of the fiber flame polished to a bead of somewhat larger diameter to help support the drop. The drop was surrounded with a retractable shield to protect it from transients when the premixed flame was ignited. Once the premixed

Table 1. Combustion Product Properties[a]

Mixture	LGP 1845[b]	Simulent Gases		
		Burner 1[d]	Burner 2[d]	Spray
Temperature (K)	2150	2295	2230	2790
Composition (% by volume)[c]				
H_2O	69.2	18.8	18.0	19.8
CO_2	12.9	9.1	8.9	--
N_2	17.4	71.2	72.6	38.3
Ar	--	--	--	40.9

[a] Computed for 10 MPa using the Gordon and McBride[20] algorithm, but effects of dissociation are small.
[b] Reactant composition (% by mass): HAN, 63.2, TEAN, 20; and H_2O, 16.8.
[c] Major species only. Minor species include CO, H_2, NO, OH and O_2.
[d] Volume flow rate of burner gases (cold) of 6.28×10^{-5} m^3/s.

flame was stabilized the shield was rapidly retracted by fusing its wire retainer so that the unbalanced pressure force on the shield forced it to one side of the pressure vessel where it was stopped by a rubber cushion.

Instrumentation. Drop diameter was measured as a function of time using backlighted high-speed motion picture photographs. The arrangement of the illuminating and camera system is illustrated in Fig. 1. The drops were backlighted by a continuous arc source, using a condensing lens to direct the light to a diffusion screen located at one of the windows. The photographs were obtained using a high-speed motion picture camera operating at roughly 1000 pictures per second which incorporated an internal timing marker.

Results and Discussion

Drop combustion at low pressures yielded very irregular variations of drop diameter as a function of time due to bubble formation and bursting within the drops. Some typical results at low pressures are illustrated in Fig. 3. Drop diameters are plotted as a function of time for five tests at 0.51 MPa with initial drop diameters in the range 580-770 μm and a 300 μm diameter bead on the quartz fiber to help support the drop. The origin of these plots is somewhat arbitrary since the motion of the retractable shield disturbed the premixed flame causing it to flap for a time; therefore, the time when the drop was finally submerged in the post flame gases was uncontrolled and variable. The results in Fig. 3 show swelling of the drop due to bubbles in the liquid in every case. The bubbles would periodically burst, carrying off some of the liquid, and occasionally the bursting of a bubble was sufficiently severe to carry off all of the liquid. At these low pressure conditions, internal reaction and bursting, with some mechanical removal of liquid caused by the bursts, appears to be the main mechanism for the reduction of the drop diameter.

The degree of drop swelling due to the presence of bubbles in the bulk liquid, and the severity of drop bursting, decreased as the pressure was increased. Some typical results at higher pressures are illustrated in Fig. 4. Drop diameter is plotted as a function of time for five representative tests at 2.1 MPa with initial drop diameters in the range 520-680 μm and a 200 μm diameter bead on the quartz fiber. As before, the time origin is arbitrary due to effects of initial disturbances on the premixed flame. All these conditions exhibited some degree of internal bubble formation, however, effects of bubbles bursting were relatively mild and complete bursting of drops was not observed at pressures of 2.1 MPa and higher.

Reduced effects of internal bubbles at high pressures appears to be largely caused by increased gas density so that a given degree of bulk liquid reaction yields a lower volume of gas: this reduces bubble sizes and growth rates which tends to reduce the severity of bursting phenomena. Counter to this is the fact that liquid surface temperatures tend to increase with increasing pressure for the present range of conditions (reaching a maximum at roughly 25 MPa):[1,2] this is expected to increase rates of bulk liquid reaction.

The time period of drop swelling, or relatively constant drop diameters, was irregular due to uncertainties concerning the time when the drop was submerged in the combustion gas environment. However, the period when the drop diameter decreased was analyzed to obtain effective drop burning rates. Plots of drop diameter as a function of time in the period where the drop diameter is decreasing are illustrated for the present test conditions in Fig. 5. The origins of these plots are arbitrary since the data has been plotted to overlap in the region where the drop diameter is decreasing. In addition, conditions where the drops burst completely at low pressures have been excluded. Results at low pressures show wide variations due to significant effects of bubble swelling and bursting but the diameter traces become more regular and repeatable at high pressures. These data were fitted to determine effective burning rates for the drops, $K_p = -dr_p/dt$: the fits are also illustrated in Fig. 5.

Present effective burning rates are plotted as a function of pressure in Fig. 6. These results are for drop diameters in the range 300-1200 μm and include effects of both internal reaction forming bubbles which burst, mechanically removing some liquid, as well as conventional gasification at the surface of the drop. This combination of effects causes the effective burning rate to be highest at the lowest pressure, where bursting dominates the process, and then to show relatively little change with pressure over most of the region considered during present tests. The strand burning results of McBratney[4,5] and Vosen[6] are also illustrated in Fig. 6. The present results are a crude extension of McBratney's[4,5] measurements of gelled propellants at higher pressures. The results of Vosen[6] are much higher than the rest of the measurements due to effects of liquid surface disturbances of burning liquid strands at high pressures, noted earlier.

Spray Combustion

Experimental Methods

Apparatus. The present spray combustion test apparatus was similar to the arrangement used by Birk and Reeves.[19] A sketch of the apparatus appears in Fig. 7. The experiments were conducted in the same chamber as the drop combustion tests. The combustion environment was produced by filling the chamber with a combustible mixture and then igniting it with two sparks to achieve the combustion gas properties summarized in Table 1 (denoted spray). The pressure of the spray tests was adjusted by varying the initial pressure of the combustible gas mixture since combustion of this gas approximated a constant volume process. The combustible gas mixture had temperatures that were somewhat greater than adiabatic combustion temperature of the monopropellant.

The spray was pressure atomized using injectors having exit diameters of 0.31, 0.58, 1.08 and 1.17 mm. The inlet of the injectors had baffles, to control any swirl in the liquid, and smooth entries, to reduce effects of cavitation. Injectors having length-to-diameter ratios of 2, 17 and 42 were considered since earlier work indicated that the degree of flow development at the injector exit influenced spray mixing properties.[2,3,13] The injectors were directed vertically upward.

A test was run by placing a propellant sample (3-4 ml) in the fuel delivery tube and filling the injector passage up to its exit. A cap was then placed over the exit to prevent gas inflow when the chamber was filled with the combustible gas mixture and further pressurized as this gas burned. The propellant flow was initiated by venting nitrogen from an accumulator into the fuel delivery tube by opening a solenoid valve. Once the pressure of the propellant was greater than the chamber pressure, the cap popped off and the resulting propellant flow generated a spray in the hot gas mixture. The process ended when all the propellant was consumed. The injector passage continued to be purged by the nitrogen flow from the accumulator for a time before the accumulator flow was ended.

Instrumentation. The combusting sprays were observed using motion picture shadowgraphs as illustrated in Fig. 7. Backlighting was provided by a flash lamp source, ca. 1 μs flash duration, which was synchronized with the camera; therefore, the image of the spray was effectively stopped on the film. The shadowgraphs were recorded with a 16 mm high-speed camera operating at roughly 1000 pictures per second, using Tri-X negative film. The camera optics yielded a 25 mm diameter field of view; therefore, it was necessary to adjust the position of the injector to observe the full length of the liquid containing region.

Since propellant combustion does not produce particulates and gas temperatures are relatively uniform in monopropellant spray flames, the boundaries of the spray were reasonably well defined -- similar to past measurements of Birk and Reeves.[19] The films were analyzed to yield mean and fluctuating time averaged liquid volume fractions, assigning dark zones to unburned liquid reactant and light zones to gaseous combustion products. For each test, 10-30 frames were available for analysis during the steady flow portion of the spray combustion process. Separating dark and light zones was somewhat subjective; and since the measurements correspond to line-of-sight projections, they are biased downstream and radially outward from correct point measurements of mean and fluctuating liquid volume fractions. Predictions were analyzed to estimate the line-of-sight biases, as discussed in the next section.

Test Conditions. Test conditions for the spray combustion tests are summarized in Table 2. Most of the injector flows correspond to fully developed flow at the injector exit, which due to the Reynolds number of the passage flow corresponds to turbulent pipe flow. Injection velocities were in the range 49-65 m/s: these conditions correspond to the atomization break-up regime, i.e., a drop-containing shear layer begins to develop at the liquid surface immediately at the injector exit.[12,13]

Theoretical Methods

Present measurements were compared with the monopropellant spray combustion analysis developed earlier in this laboratory.[1,3] Drop trajectory calculations were also carried out in order to help assess effects of separated-flow phenomena. Both analyses are described in the following.

Spray Analysis. The main features of the spray analysis will be only briefly described in the following, original sources should be consulted for details.

The analysis involves use of the LHF approximation of multiphase flow theory[11-13] and the thin laminar flamelet approximation of premixed turbulent flame theory.[14,15] Turbulent mixing was treated using a Favre-averaged turbulence model.[14-17] This approach provides a useful limit since both multiphase and chemical reaction phenomena are controlled by turbulent mixing which minimized the empiricism needed for predictions, e.g., initial drop size and velocity distributions, chemical kinetic properties, etc., are not needed to define the problem. The main limitation of the LHF approximation is that its use generally tends to overestimate the rate of development of sprays, particularly in dilute-spray regions far from the injector exit.[11-13] However, Ruff et al.[13] find that the LHF approach, using the present turbulent-mixing model, provided reasonably good estimates of mixing properties in the near-injector dense-spray region of nonevaporating pressure-atomized sprays in the atomization breakup regime -- conditions that are representative of present tests.

The thin laminar flamelet approximation implies that heterogeneous monopropellant flames cover all liquid surfaces. Except for very near the liquid surface, the liquid is at the same state as in the injector while beyond the outer edge of the thin flame the gas has uniform properties equivalent to adiabatic flame conditions noted in Table 1. Under the LHF approximation, relative velocities between the phases (slip) are neglected.

Other major assumptions of the analysis are as follows: (1) steady (in the mean) axisymmetric flow with no swirl; (2) low Mach numbers with negligible potential and kinetic energy changes, and negligible viscous dissipation; (3) boundary-layer approximations apply; (4) negligible effects of radiant energy exchange; (5) equal exchange coefficients of all species and heat; and (6) high Reynolds numbers, so that laminar transport is negligible in comparison to turbulent transport. Justification of these assumptions is presented in Refs. 1 and 3.

Under these assumptions, flow properties can be found by solving governing equations for conservation of mass, momentum and reaction progress variable, in conjunction with second-order turbulence model equations for turbulence kinetic energy and its rate of dissipation.[14,15] The formulation, all empirical constants used in the turbulence model, and the method of solution, can be found in Ref. 3.

The predictions were also used to estimate potential effects of line-of-sight biasing on the measured distributions of liquid volume fractions using a stochastic approach developed for radiation calculations in this laboratory.[21] Knowing the time-averaged probability density function of the reaction progress variable along paths through the flow, the reaction progress variable was simulated for a series of statistically-independent eddies along the path. Counting the presence of any liquid in the path as a condition which would block the light, giving a dark image on the film, yielded estimates of time averaged mean and fluctuating liquid volume fractions for the path. This procedure has not been calibrated using known flows, however, it does provide at least a qualitative indication of potential effects of line-of-sight bias.

Table 2. Summary of Combusting Spray Test Conditions

Diameter (mm)	L/d	Flow Type[a]	Amb. Pres. (MPa)	Pressure Drop (MPa)	Inj. Velocity[b] (m/s)	Re[c]	Oh[d]	We_f[e]
Radial Measurements:								
1.17	17	FDF	3.11	2.02	52.7	12600	0.021	70700
1.17	17	FDF	7.07	1.79	49.3	11800	0.021	62400
1.17	17	FDF	9.10	1.81	49.7	11900	0.021	63300
1.08	2	SF	6.83	1.93	51.4	11400	0.022	62200
0.58	42	FDF	3.19	2.07	53.2	6300	0.030	35800
0.58	42	FDF	6.15	2.76	61.6	7300	0.030	47900
Axial Measurements:								
0.58	42	FDF	3.22	2.33	56.6	6700	0.030	40400
0.58	42	FDF	6.16	1.81	49.5	5900	0.030	30900
0.58	42	FDF	8.99	2.14	54.3	6400	0.030	37100
0.31	42	FDF	6.51	3.05	64.8	4000	0.041	27800

[a]FDF = fully developed flow; SF = slug flow.

[b]Unity flow coefficient.

[c]$Re = \rho_f u_o d/\mu_f$, $\mu_f = 0.0071$ kg/ms.

[d]$Oh = \mu_f / \sqrt{\rho_f d \sigma}$, $\sigma = 0.0669$ kg/s^2.

[e]$We_f = \rho_f u_o^2 d/\sigma$.

Drop Trajectory Analysis. Direct assessment of the approximations of the LHF approach for the monopropellant sprays was undertaken using drop trajectory calculations, similar to the approach used by Shearer et al.[22] and Mao et al.[23] for nonpremixed spray flames. These calculations were limited to drops moving along the axis of the spray. The drops were assumed to be always in contact with the gas phase which was taken to have the properties summarized in Table 1. Estimates of the gas velocity variation along the axis were obtained from the LHF analysis.

Drop trajectory calculations were limited to deterministic calculations, ignoring effects of turbulence/drop interactions; therefore, mean gas velocities from the LHF analysis were used in the governing equations for drop motion. Drops were assumed to be surrounded by gas immediately at the injector exit, ignoring the all-liquid core present in these sprays.[13] Effects of drop heat-up were also ignored: the drop radius was assumed to decrease throughout the entire trajectory at 10 mm/s -- based on the results of Fig. 6 for the present test range. This high burning rate implies that the decomposition flame is located near the drop surface, well within the boundaries of the flow field around the drop; therefore, gas-phase properties used to estimate drop drag were taken to be ambient gas properties and effects of forced convection or drop burning rates were ignored. Other aspects of the analysis were similar to Refs. 22 and 23: the flow field around the drop was assumed to be quasi-steady; virtual mass, pressure-gradient, Basset history and gravitational forces were ignored; swelling of the drops was ignored; and drop drag was estimated using the standard drag correlation for solid spheres.

Under these assumptions, the governing equations of drop motion along the axis are as follows:

$$dx_p/dt = u_p \tag{1}$$

$$dd_p/dt = -2\,K_p \tag{2}$$

$$du_p/dt = -3\rho_g\,C_D\,|\,u_p - \bar{u}\,|\,(u_p - \bar{u})/4 \tag{3}$$

where

$$C_D=24\,(1+Re_p^{2/3}/6)/Re_p,\ Re_p \le 1000;\ C_D=0.44,\ Re_p>1000 \tag{4}$$

The initial condition is $u_p = u_o$, $d_p = d_{po}$ and $x_p = 0$ at $t = 0$. Equations (1) - (3) were integrated using a Runge-Kutta algorithm.

Results and Discussion

Due to strong background lighting, it was not possible to determine that ignition had taken place from flame luminosity. Nevertheless, ignition was readily identified from the pressure trace: inert liquid (like water or unignited monopropellant spray liquid) caused the hot combustion products of the premixed gas flame to be quenched which resulted in a rapid reduction of the chamber pressure; in contrast, energy release from the combusting monopropellant spray caused an increase of chamber pressure in the period when the propellant was flowing. It was possible to consistently ignite the spray at pressures as low as 2.7 MPa, however, the bulk of spray measurements were obtained at pressures of 3-9 MPa.

Measured and predicted time-averaged liquid volume fractions along the axis, $\bar{\alpha}_{fc}$, are plotted as a function of normalized distance from the injector exit, x/d, in Fig. 8. Both present measurements and those of Birk and Reeves[19] are shown on the plot. Predictions include direct values of $\bar{\alpha}_{fc}$ as well as results allowing for line-of-sight bias, as noted earlier.

Test conditions used by Birk and Reeves[19] were similar to present test conditions, except that injector L/d were in the range 1.2-2.4 and the injector inlet was not rounded (see Lee et al.[3] for a sketch of the injectors), and injector pressure drops were 1.5-2.0 times higher than the present study. The motion picture shadowgraphs of both investigations were obtained in a similar manner and were analyzed in this laboratory. Each set of experimental results also exhibits a significant degree of internal consistency and repeatability when plotted in the manner of Fig. 8. Finally, pressure traces indicated that measurements were obtained for combusting sprays for both studies. Nevertheless, present measurements exhibit a much longer liquid-containing region than those of Birk and Reeves,[19] e.g., $\bar{\alpha}_{fc} = 0.5$ at x/d roughly 150 and 25 for the two sets of measurements. Specific reasons for these differences are not obvious since so many features of the two studies were the same, however, changes in injection properties offer the most plausible explanation. In particular, the sharper injector inlet used by Birk and Reeves[19] could have caused cavitation in the injector passage resulting in a more finely atomized spray with a rapid rate of radial spread. Similarly, the injector used by Birk and Reeves[19] did not have a flow straightener and swirl induced in the injector flow passage could have resulted in unusually high radial spread rates; although the fuel-injection system only involved rectilinear motion and doesn't appear to be fundamentally prone to induce swirl. Finally, Birk and Reeves[19] employed somewhat higher injector pressure drops which would be expected to yield smaller drop sizes in the spray; nevertheless, spray conditions for both investigations were in the atomization breakup regime and the pressure drop increase doesn't appear to be sufficient to explain the differences seen in Fig. 8 based on the relatively small effect of pressure drop variations observed during this investigation. In any event, extensive rechecking of measurements using the present injectors could not reproduce the results of Birk and Reeves.[19]

Present measurements in Fig. 8 are roughly similar (in terms of x/d) at all test conditions, with the downstream limit of the liquid-containing region at x/d ca. 350. Since these results involve a range of pressures and injector diameters, this behavior suggests a mixing-controlled process supporting the use of LHF analysis -- a conclusion reached in Ref. 3, based on the measurements of Birk and Reeves.[19] Closer examination of the data, however, reveals trends that suggest significant separated-flow effects. First of all, results for the 0.31 mm diameter injector consistently exhibit higher values of $\bar{\alpha}_{fc}$ at a particular x/d than the 0.58 mm diameter injector. This is a separated-flow property since drop diameters are not strongly affected by injector diameters while drops of a particular size must penetrate a certain distance in order to disappear: this causes in a tendency for penetration distances, x, to be constant for separated flows rather than x/d.[11] Another effect is that $\bar{\alpha}_{fc}$ at a particular x/d is lower for a chamber pressure of 8.99 MPa than the other pressures considered for the 0.58 mm diameter injector: this behavior parallels the effective burning rate results of Fig. 6 where drop burning rates at 9 MPa are higher than for pressures in the range 3-6 MPa, which are roughly the same. A final effect is that use of long and short L/d injectors yielded roughly the same results while mixing-controlled flows would result in much faster mixing rates for the long L/d injector.[13]

Predictions illustrated in Fig. 8 are for fully-developed flow at the injector exit, which corresponds to the bulk of present test conditions. Effects of ambient pressure, injector diameter and injector Reynolds number had little effect on the predictions; therefore, only single lines are shown for results with and without the line-of-sight bias correction. Comparing predictions with and without the line-of-sight bias correction indicates significant effects of bias for intermediate values of $\bar{\alpha}_{fc}$; however, predictions of the downstream end of the liquid-containing region are not strongly influenced by the bias.

In view of the bias uncertainties, the predictions illustrated in Fig. 8 are in fair agreement with the measurements of Birk and Reeves.[19] This observation prompted earlier encouragement concerning the value of the LHF and thin laminar flamelet approximations for analyzing flows of this type. However, comparison of predictions with present measurements implies that use of the LHF approximation causes the rate of development of the spray to be substantially overestimated, in agreement with most other evaluations of the LHF approximation for sprays.[11-13]

Radial profiles of time-averaged liquid volume fractions at various distances from the injector are illustrated in Fig. 9. All measurements shown in the figure were obtained during the present investigation. Predictions shown on the figure account for line-of-sight bias and are for fully-developed flow at the injector exit. Similar to results along the axis, predictions were relatively independent of test conditions and only a single line is shown for each streamwise position. Results ignoring line-of-sight bias are narrower than the plots illustrated in Fig. 9, however, the outer extent of the liquid-containing region is about the same.

Similar to results along the axis, the measured radial profiles are crudely similar for all the test conditions when plotted in the manner of Fig. 9. In terms of r/x, the radial similarity variable of turbulent jets, the liquid-containing region extends to 0.05-0.07, rather than 0.15 which is the typical width based on scalar properties in turbulent jets. Predictions provide a fair estimate of flow widths near the injector exit but progressively fail with increasing distance from the injector exit -- tending to overestimate the rate of development of the flow. This behavior is similar to other evaluations of the use of the LHF approximation for both nongasifying and gasifying sprays.

Potential effects of separated flow are examined directly by the drop trajectory computations illustrated in Fig. 10. Drop velocities and diameters along the axis are plotted as a function of distance from the injector for an ambient pressure of 10 MPa. Predictions of velocities along the axis from the LHF analysis are also illustrated on the plot, as a reference. Results are shown for initial drop diameters of 10, 20, 100 and 200 μm; drops much larger than 200 μm would be subject to secondary breakup due to excessively-high drop Weber numbers.[12] Unlike LHF predictions, drop trajectory calculations depend on the initial injector diameter, as noted earlier: the results illustrated in Fig. 10 are for an injector diameter of 1.00 mm.

The results illustrated in Fig. 10 clearly show significant effects of separated flow. The LHF predictions exhibit a decay of velocity beyond the potential-core-like region which is roughly inversely proportional to pressure -- similar to single-phase jets. Due to the small diameter of the injector, this results in a rapid deceleration rate. Only the smallest drops (initial diameters of 10 μm or less) have sufficiently fast response to approach the velocities of the continuous phase throughout most of their trajectory. With increasing drop size, the drops progressively overshoot the velocity of the continuous phase and only approach it again toward the end of their life, when they become very small. Similarly, the drops pass beyond the end of the liquid-containing region estimated by the LHF analysis (taken to be $\alpha_{fc} \geq 10^{-4}$ since liquid volume fraction never formally reaches zero in the LHF analysis due to its statistical treatment). Use of the drop burning rate estimates of Fig. 6, however, yields drop trajectories extending to x/d ca. 300 for initial drop diameters of 200 μm. This is comparable to present measurements of the extent of the liquid-containing region suggesting that the results of the drop trajectory calculations are at least reasonable.

Taken together, the results of Figs. 8-10 suggest significant effects of separated flow for combusting HAN-based monopropellant sprays over the present range of test conditions. In view of the relatively modest variation of burning rate with pressure seen in Fig. 6, the insensitivity of drop drag properties to pressure,[11,12] and the relatively high critical combustion pressure of HAN-based monopropellants (ca. 250 MPa[1,2]) it is likely that separated-flow phenomena are important for combusting HAN-based monopropellant sprays for most of their range of application.

Conclusions

The present study involved measurements of the combustion properties of the HAN-based monopropellant LGP 1845, both as drops and sprays in combustion gas environments at pressures of 0.2-9 MPa. The spray measurements, and drop trajectory calculations based on the present drop burning rate measurements, were used to evaluate earlier analysis of combusting monopropellant sprays based on the locally homogeneous flow and thin laminar flamelet approximations, due to Lee et al.[1,3] Major conclusions of the study are as follows:

1. Measurements yielded effective drop burning rates of ca. 10 mm/s for drop diameters of 300-1200 μm and pressures of 0.2-7 MPa. The effective drop burning rate involved both reaction within the bulk liquid causing bubble formation and bursting, dominating the process at low pressures; and conventional gasification from the drop surface, dominating the process at high pressures: taken together, these effects cause burning rates to be relatively independent of pressure over the present test range.

2. Present measurements of drop burning rates at pressures of 0.7-7 MPa are generally consistent with earlier strand burning rate measurements of gelled propellants due to McBratney[4,5] at pressures greater than 10 MPa.

3. Present measurements exhibited a much larger liquid containing region for combusting sprays at pressures of 3-9 MPa than the earlier measurements of Birk and Reeves[19] even though test conditions and methods of data analysis were similar, e.g., $\bar{\alpha}_{fc} = 0.5$ at x/d roughly 150 and 25 for the two sets of experiments. Reasons for these differences have not been firmly established but different injector passage conditions, possibly leading to effects of cavitation, swirl and finer atomization for the measurements of Ref. 19, have been advanced as a possible explanation.

4. While earlier evaluation of analysis using the LHF and thin laminar flamelet approximations appeared promising based on the measurements of Birk and Reeves;[19] current findings suggest that this approach substantially overestimates the rate of development of the flow which is consistent with recent findings for other pressure-atomized spray processes.[11-13] Separated flow phenomena appear to be important combusting for HAN-based monopropellant sprays over much of their range of application.

Acknowledgements

This research was sponsored by the Army Research Office and the U.S. Army Armament Research, Development and Engineering Center, Picatinny Arsenal, NJ under Contract No. DAAL03-86-K-0154.

References

[1]Faeth, G. M., Lee, T.-W. and Kounalakis, M. E., "Mixing and Thermodynamic Critical Phenomena of Combusting Monopropellant Sprays," Proceedings of the 24th JANNAF Combustion Meeting, October 1987.

[2]Kounalakis, M. E., and Faeth, G. M., "Combustion of HAN-Based Liquid Monopropellants Near the Thermodynamic Critical Point," Combust. Flame, in press.

[3]Lee, T.-W., Gore, J. P., Faeth, G. M., and Birk, A., "Analysis of Combusting High-Pressure Monopropellant Sprays," Combust. Sci. and Tech., Vol. 57, 1988, pp. 95-112.

[4]McBratney, W. F., "Windowed Chamber Investigation of the Burning Rate of Liquid Monopropellants for Guns," Report No. ARBRL-MR-03018, Ballistic Research Laboratory, Aberdeen Proving Ground, 1980.

[5]McBratney, W. F., "Burning Rate Data LGP 1845," Report No. ARBRL-MR-03128, Ballistic Research Laboratory, Aberdeen Proving Ground, 1981.

[6]Vosen, S. R. "The Burning Rate of HAN-Based Liquid Propellants," Twenty-Second Symposium (International) on Combustion, The Combustion Institute, Pittsburgh, in press.

[7]Zhu, D. L. and Law, C. K., "Aerothermochemical Studies of Energetic Liquid Materials: 1. Combustion of HAN-Based Liquid Gun Propellants Under Atmospheric Pressure," Combust. Flame, Vol. 70, 1987, pp. 333-342.

[8]Beyer, R. A., "Atmospheric Pressure Studies of Liquid Monopropellant Drops in Hot Flows," Technical Report BRL-TR-2768, Ballistic Research Laboratory, Aberdeen Proving Ground, 1986.

[9]Beyer, R. A., "Single Droplet Studies in a Hot, High Pressure Environment," Technical Report BRL-TR-2900, Ballistic Research Laboratory, Aberdeen Proving Ground, 1988.

[10]Beyer, R. A., and Teague, M. W., "Studies of Single Liquid Propellant Drops in Hot, High Pressure Environments," 22nd JANNAF Combustion Meeting, CPIA Publication 457, Vol. 2, p. 429, 1986.

[11]Faeth, G. M., "Evaporation and Combustion in Sprays," Prog. Energy Combust. Sci., Vol. 9, 1983, pp. 1-76.

[12]Faeth, G. M., "Mixing, Transport and Combustion in Sprays," Prog. Energy Combust. Sci., Vol. 13, 1987, pp. 293-345.

[13]Ruff, G. A., Sagar, A. D. and Faeth, G. M., "Structure and Mixing Properties of Pressure-Atomized Sprays," AIAA J., in press.

[14]Bray, K.N.C., "Interaction Between Turbulence and Combustion," Seventeenth Symposium (International) on Combustion, The Combustion Institute, Pittsburgh,, 1978, pp. 223-233.

[15]Bray, K.N.C., "Turbulent Flows with Premixed Reactants," Turbulent Reacting Flows (P. A. Libby and F. A. Williams, Eds.), Springer, Berlin, 1980, pp. 115-135.

[16]Bilger, R. W., "Turbulent Jet Diffusion Flames," Prog. Energy Combust. Sci., Vol. 1, 1976, pp. 87-109.

[17]Jeng, S. M. and Faeth, G. M., "Species Concentrations and Turbulence Properties in Buoyant Methane Diffusion Flames," J. Heat Trans., Vol. 106, 1984, pp. 721-727.

[18]Lockwood, F. C. and Naguib, A. S., "The Prediction of Fluctuations in the Properties of Free, Round Jet, Turbulent Diffusion Flames," Combust. Flame, Vol. 24, 1975, pp. 109-124.

[19]Birk, A. and Reeves, P., "Annular Liquid Propellant Jets — Injection, Atomization and Ignition," Report No. BRL-TR-2780, Ballistic Research Laboratory, Aberdeen Proving Ground, 1987.

[20]Gordon, S. and McBride, B. J., "Computer Program for Calculation of Complex Chemical Equilibrium Compositions, Rocket Performance, Incident and Reflected Shocks and Chapman-Jouguet Detonations," NASA Report SP-273, Washington, 1971.

[21]Faeth, G. M., Gore, J. P., Chuech, S. G. and Jeng, S. M., "Radiation from Turbulent Diffusion Flames," Ann. Rev. Num. Fluid Mech. and Heat Trans., Vol. 2, 1988, pp. 1-38.

[22]Shearer, A. J., Tamura, H. and Faeth, G. M., "Evaluation of a Locally Homogeneous Flow Model of Spray Evaporation," J. Energy, Vol. 3, September-October 1979, pp. 271-278.

[23]Mao, C.-P., Wakamatsu, Y. and Faeth, G. M., "A Simplified Model of High Pressure Spray Combustion," Eighteenth Symposium (International) on Combustion, The Combustion Institute, Pittsburgh, 1981, pp. 337-347.

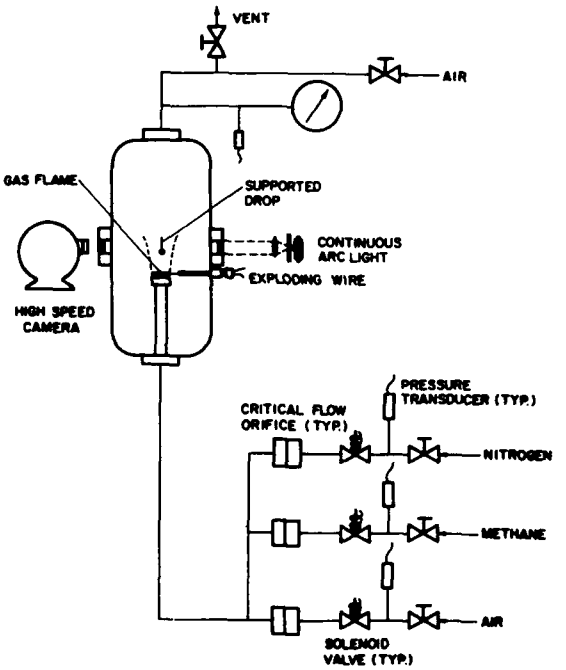

Fig. 1. Sketch of the drop combustion apparatus.

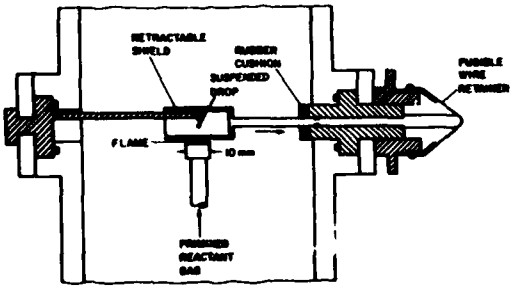

Fig. 2. Sketch of the drop support assembly.

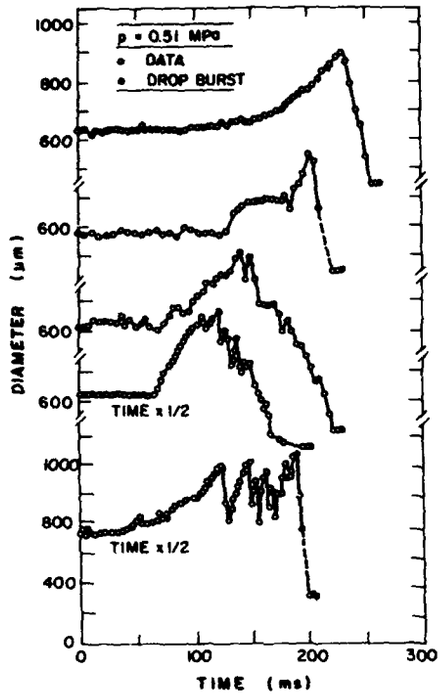

Fig. 3. Drop diameter histories at 0.51 MPa.

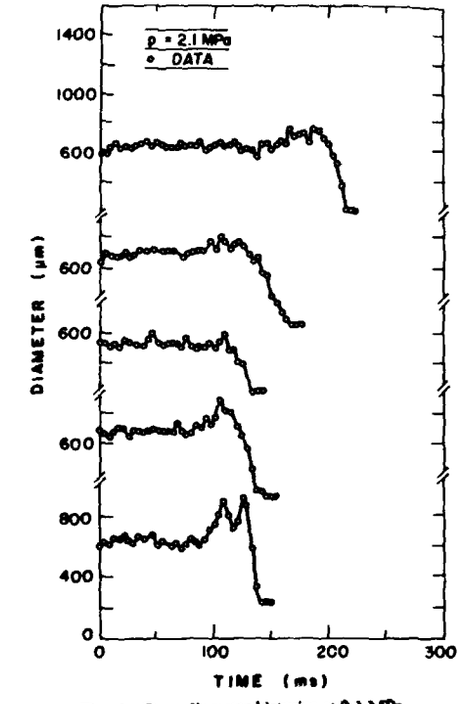

Fig. 4. Drop diameter histories at 2.1 MPa.

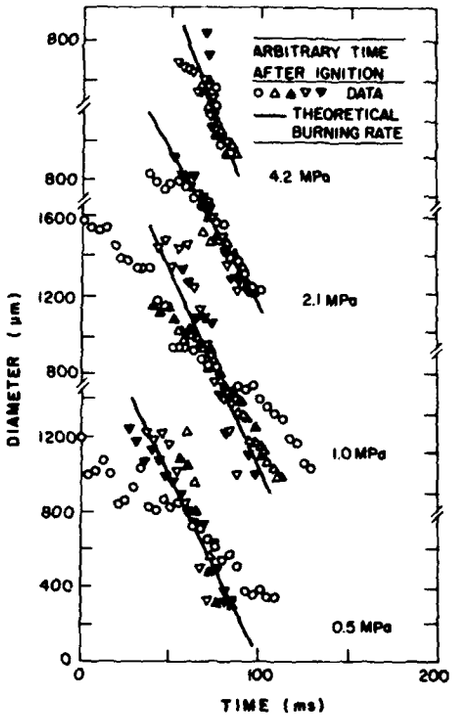

Fig. 5. Drop diameter histories in the combustion period.

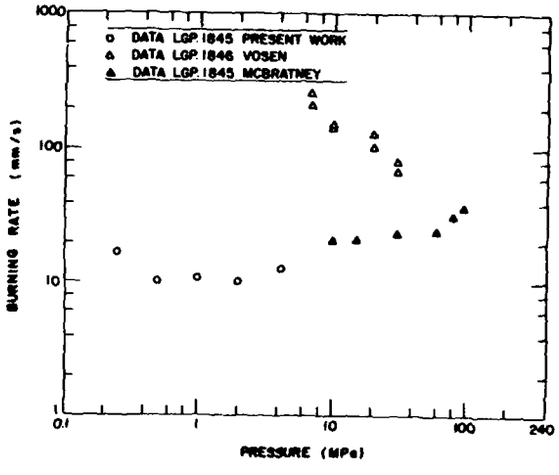

Fig. 6. Apparent drop burning rates as a function of pressure.

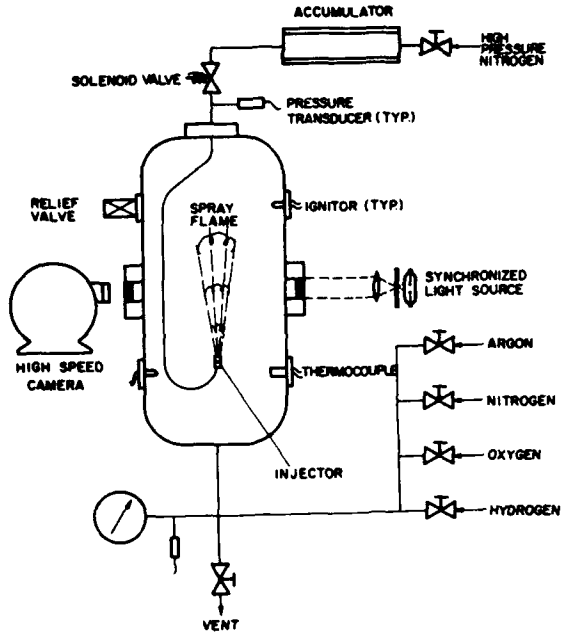

Fig. 7. Sketch of a spray combustion apparatus.

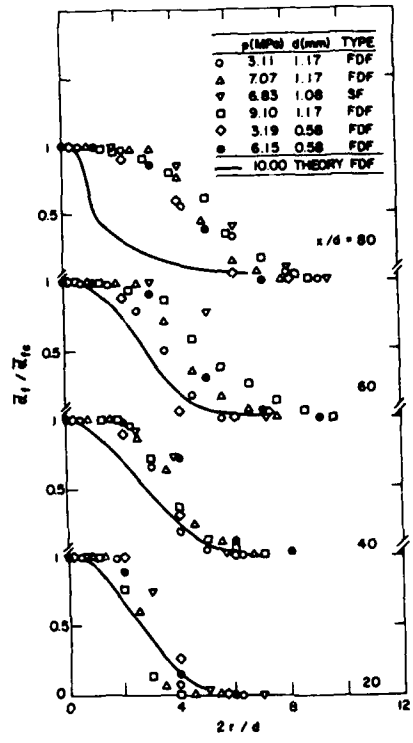

Fig. 9. Radial profiles of time-averaged liquid volume fractions. Predictions with line-of-sight bias correction.

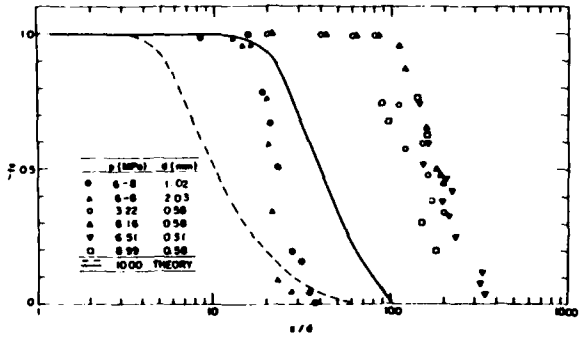

Fig. 8. Time-averaged liquid volume fractions along axis. Open symbols, present study; closed symbols, Birk and Reeves. Dashed and solid lines are predictions without and with line-of-sight bias correction.

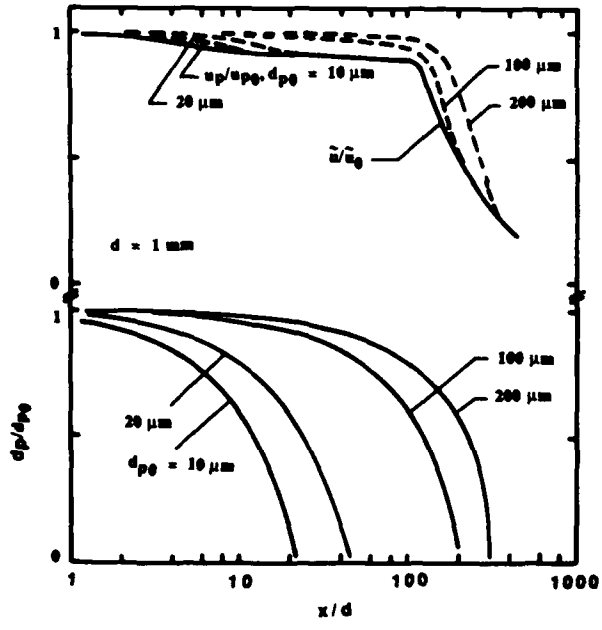

Fig. 10 Drop trajectory properties along axis. Note that $\bar{\omega}_{fc} = 10^{-4}$ at x/d = 220 for the LHF calculation.